Chapter 7

Nonlinear Transformations and Radar Detector Design

Graham V. Weinberg

Additional information is available at the end of the chapter

http://dx.doi.org/10.5772/65677

Abstract

A nonlinear transformation is introduced, which can be used to compress a series of random variables. For a certain class of random variables, the compression results in the removal of unknown distributional parameters from the resultant series. Hence, the application of this transformation is investigated from a radar target detection perspective. It will be shown that it is possible to achieve the constant false alarm rate property through a simple manipulation of this transformation. Due to the effect the transformation has on the cell under test, it is necessary to couple the approach with binary integration to achieve reasonable results. This is demonstrated in an X-band maritime surveillance radar detection context.

Keywords: transformations, random variable properties, radar detection, mathematical statistics, radar

1. Introduction

The fundamental problem to be examined in this chapter is the detection of targets embedded within the sea surface, from an airborne maritime surveillance radar. Artifacts of interest could be lifeboats or aircraft wreckage resulting from aviation or maritime disasters. From a military perspective, one may be interested in the detection and tracking of submarine periscopes. Another scenario may be the detection of illegal fishing vessels or small boats used for smuggling of people or contraband. An airborne maritime surveillance radar has a difficult task in the detection of such objects from high altitude, while surveying a very large surveillance volume.

Such radars operate at X-band and are high resolution, and as such are affected by backscattering from the sea surface, which is referred to as clutter. This backscattering tends to mask small targets and makes the surveillance task extremely difficult. One of the major issues with the design of radar detection schemes is the minimization of the detection of false tar-

gets, while maximizing the detection of real targets. As a statistical hypothesis test, one can apply the Neyman-Pearson Lemma to produce a decision rule that achieves these objectives. However, in many cases, such a decision rule requires clutter model parameter approximations as well as estimates of the target strength based upon sampled returns. An issue, well known within the radar community, is that small variations in the clutter power level can result in huge increases in the number of false alarms. Since clutter power is a function of the underlying clutter model's parameters, approximations of the latter will have an inevitable effect on the former. Hence a large body of research has been devoted to designing radar detection strategies that maintain a fixed level of false alarms. A detector that achieves this objective is said to have the constant false alarm rate (CFAR) property [1].

In order to maintain a fixed rate of false alarms, sliding window decision rules were examined in early studies of radar detection strategies [2–6]. These investigations have been extended to account for different clutter models and to address issues with earlier detector design in a number of subsequent analyses [7–15]. Such decision rules can be formulated as follows. Suppose that the statistic Z is the return to be tested for the presence of a target. Let $Z_1, Z_2, \ldots, Z_N$ be N statistics from which a measurement of the level of clutter is taken, via some function $f = f(Z_1, Z_2, \ldots, Z_N)$. Then a target is declared present in the case where Z is larger than a constant times f. The constant is selected so that in ideal scenarios, the false alarm rate remains fixed. It is generally assumed that the clutter statistics are independent and identically distributed in ideal settings, and also independent of the statistic Z. This can be formulated as a statistical hypothesis test by letting H_0 be the hypothesis that the cell under test (CUT) statistic Z does not contain a target, and H_1 the alternative that it contains a target embedded within clutter. Then the test is written

$$Z \underset{H_0}{\overset{H_1}{\gtrless}} \tau f(Z_1, Z_2, \ldots, Z_N) \tag{1}$$

where $\tau > 0$ is the threshold constant and the notation used in Eq. (1) means that H_0 is rejected when $Z > \tau f(Z_1, Z_2, \ldots, Z_N)$. The probability of false alarm is given by

$$\text{Pfa} = \mathbb{P}\left(Z > \tau f(Z_1, Z_2, \ldots, Z_N) \,\middle|\, H_0\right). \tag{2}$$

If τ can be determined, for a specified Pfa in Eq. (2), such that it is independent of clutter parameters, then the decision rule in Eq. (1) will be able to maintain the CFAR property in ideal scenarios. In practical radar systems, a detection scheme such as in Eq. (1) can be run across the data returns sequentially to allow binary decisions on the presence of targets to be made, which are then passed to a tracking algorithm. A comprehensive examination of such detection processes is included in [1].

This chapter examines an alternative approach to achieve the CFAR property, based upon a nonlinear transformation that is used to compress the original clutter sequence. The consequence of this is that the resulting transformed series of random variables will have a fixed clutter power level and so permits a CFAR detector to be proposed. It is then shown how this transformation can be used to produce a practical radar detection scheme.

The chapter is organized as follows. Section 2 introduces the nonlinear mapping and formulates a decision rule. Section 3 specializes this to the case of Pareto distributed sequences, since

http://dx.doi.org/10.5772/65677

the Pareto model is suitable for X-band maritime surveillance radar clutter returns. Section 4 demonstrates detector performance in homogeneous clutter, while Section 5 applies the decision rules directly to synthetic target detection in real X-band radar clutter.

2. Transformations and decision rule

2.1. Mapping

In X-band maritime surveillance radar, the Pareto distribution has become of much interest as a clutter intensity model due to its validation relative to real radar clutter returns [16–18]. This model arises as the intensity distribution of a compound Gaussian model with inverse Gamma texture. Consequently, the Pareto distribution fits into the currently accepted radar clutter model phenomenology [19]. Hence, there have been a number of recent advances in the design of CFAR processes under a Pareto clutter model assumption [20–25].

A random variable X has a Pareto distribution [26] with shape parameter $\alpha > 0$ and scale parameter $\beta > 0$ if its cumulative distribution function (cdf) is

$$F_X(t) := \mathbb{P}(X \leq t) = 1 - \left(\frac{\beta}{t}\right)^{\alpha}, \tag{3}$$

for $t \geq \beta$. The density of X follows by differentiation of Eq. (3). In order to ensure the existence of the first two moments, it is usually assumed that $\alpha > 2$, which is an assumption that has been validated in fits of this model to real data [18]. This Pareto model possesses what is referred to as a duality property in Ref. [20]. To introduce this, recall that if Y is an Exponential random variable with unity mean, its cdf is given by

$$F_Y(t) = 1 - e^{-t} \tag{4}$$

for $t \geq 0$. Then it can be shown that the Pareto model in Eq. (3) can be related to Eq. (4) via the random variable relationship

$$X = \beta e^{\alpha^{-1}Y}. \tag{5}$$

Other random variables of interest in radar signal processing, such as the Weibull, can also be expressed in a form similar to Eq. (5). Hence, for the purposes of generality, suppose $\{X_j, j \in \mathbb{N} := \{0, 1, 2, \ldots\}\}$ is a sequence of homogeneous random variables with common support and that θ_1 and θ_2 are two fixed real constants. Define a sequence of random variables $\{Z_j, j \in \mathbb{N}\}$ by

$$Z_j = \theta_1 X_j^{\theta_2}. \tag{6}$$

The sequence produced via Eq. (6) is a generalization of the Pareto model (3). Next define a nonlinear mapping $\zeta : \mathbb{R}^+ \times \mathbb{R}^+ \times \mathbb{R}^+ \times \mathbb{R}^+ \to \mathbb{R}^+ \cup \{0\}$ by

$$\zeta(x_1, x_2, x_3, x_4) = \left|\frac{\log(x_1) - \log(x_2)}{\log(x_3) - \log(x_4)}\right|, \tag{7}$$

where each $x_j > 0$, $x_3 \neq x_4$ and $\mathbb{R}^+$ is the positive real numbers. Then the following result is relatively easy to prove:

Lemma 2.1 *Suppose* $\{Z_j, j \in \mathbb{N}\}$ *is a sequence of random variables defined via Eq. (6). Then the sequence* $\{W_j, j \in \mathbb{N}\}$ *with* $W_j := \zeta(Z_j, Z_{j+1}, Z_{j+2}, Z_{j+3})$ *does not depend on* θ_1 *and* θ_2.

The proof of Lemma 2.1 is now outlined. Supposing that Z_j, Z_{j+1}, Z_{j+2} and Z_{j+3} are represented in the form defined via Eq. (6) it follows that

$$\begin{aligned} W_j &= \left| \frac{\log\left(\theta_1 X_j^{\theta_2}\right) - \log\left(\theta_1 X_{j+1}^{\theta_2}\right)}{\log\left(\theta_1 X_{j+2}^{\theta_2}\right) - \log\left(\theta_1 X_{j+3}^{\theta_2}\right)} \right| \\ &= \left| \frac{\theta_2 \log\left(X_j\right) - \theta_2 \log\left(X_{j+1}\right)}{\theta_2 \log\left(X_{j+2}\right) - \theta_2 \log\left(X_{j+3}\right)} \right| \\ &= \left| \frac{\log\left(X_j\right) - \log\left(X_{j+1}\right)}{\log\left(X_{j+2}\right) - \log\left(X_{j+3}\right)} \right|, \end{aligned} \tag{8}$$

where properties of the logarithmic function have been utilized. Since Eq. (8) does not depend on θ_1 and θ_2, the proof is completed.

Lemma 2.1 suggests that if the original sequence of random variables is processed in 4-tuples, the compressed sequences' statistical structure is only dependent on the random variables X_j. Observe that the Lemma does not require an independence assumption. Thus if sequence $\{X_j\}$ has no unknown statistical parameters, the process generated by Eq. (7) also has no unknown parameters. This suggests that processing of a data sequence in terms of 4-tuples may be an effective may in which to achieve the CFAR property. The next subsection clarifies this.

2.2. Decision rule

In order to propose a decision rule exploiting the transformation introduced in Lemma 2.1, it is necessary to focus first on a series of four returns. Hence, suppose we have a CUT statistic Z, and three clutter measurements are available, denoted Z_1, Z_2 and Z_3. Let H_0 be the hypothesis that the CUT contains no target, and H_1 the hypothesis that it does contain a target embedded within clutter. Then, based upon Eq. (7), a linear threshold test takes the form

$$\zeta(Z, Z_1, Z_2, Z_3) \underset{H_0}{\overset{H_1}{\gtrless}} \tau, \tag{9}$$

where $\tau > 0$ is the threshold. Based upon Lemma 2.1 if the clutter is modelled by Eq. (6), then it is clear that under H_0, the Pfa of the test in Eq. (9) will not depend on θ_1 or θ_2, implying it is CFAR with respect to these parameters. Furthermore, an auxiliary motivation for defining a linear threshold detector such as Eq. (9) is that in the cases where it is assumed that one has *a priori* knowledge of clutter parameters, linear threshold detectors are ideal, or asymptotically optimal, and hence provide the maximum probability of detection within the class of sliding window decision rules [27].

http://dx.doi.org/10.5772/65677

The test in Eq. (9) can also be re-expressed in terms of the preprocessed clutter statistics. In particular, it can be shown to be equivalent to rejecting H_0 if

$$\begin{aligned} &Z > Z_1 e^{\tau|\log(Z_2)-\log(Z_3)|} \\ &\text{or} \\ &Z > Z_1 e^{\tau|\log(Z_2)-\log(Z_3)|} \end{aligned} \tag{10}$$

with the appropriate choice for τ, which can be determined from the corresponding Pfa expression for Eqs. (9) or (10).

Observe that this test is not of the usual form found in the radar signal processing literature, since it compares a CUT with a measurement of clutter based upon three statistics, and not upon a sample of predetermined size. This will be discussed subsequently in terms of practical implementation of the test in Eq. (10). The next section discusses the application of Eq. (10) to the Pareto clutter case, enabling the determination of τ.

3. Specialization to the Pareto Clutter model

3.1. Distributions under H_0

Since the motivation of the work developed here is the design of radar detection schemes for maritime surveillance radar, the results of the previous section are specialized to the Pareto case. In order to apply Lemma 2.1, it is necessary to determine the distribution of the resultant sequence produced by ζ under H_0. The following is the key result:

Corollary 3.1 *In the case where the sequence of random variables in Lemma 2.1 is Pareto distributed and independent, the cdf of the sequence processed by ζ is given by*

$$F_P(t) = \frac{t}{t+1}, \tag{11}$$

for $t \geq 0$.

This can be recognized as a Pareto distribution, with support the nonnegative real line and shape and scale parameter unity. More specifically, $P = X + 1$, where X has density (3) with $\alpha = \beta = 1$. This illustrates the cost of the nonlinear transformation approach: although the resultant series of clutter has no unknown clutter parameters, it is from a distribution with no finite moments. The independence assumption is adopted for analytical tractability and is consistent with the assumption that independent and identically distributed clutter returns are available, as in the formulation of the test in Eq. (1).

To prove Corollary 3.1, suppose that η_1 and η_2 are two independent random variables with cdf (4). Then by analyzing the difference $\eta_1 - \eta_2$, it can be shown that it has cdf

$$F_{\eta_1-\eta_2}(t) = \begin{cases} 1-\frac{1}{2}e^{-t}, & \text{for } t \geq 0 \\ \frac{1}{2}e^{t} & \text{for } t < 0, \end{cases} \tag{12}$$

which is that of a Laplace distribution. Then it follows that

$$F_{|\eta_1-\eta_2|}(t) = \mathbb{P}(-t \le \eta_1 - \eta_2 \le t) = 1 - e^{-t}, \tag{13}$$

where Eq. (12) has been applied, and $t > 0$. Thus the modulus of the difference is also exponentially distributed with unit mean.

Supposing that κ_1 and κ_2 are two independent random variables with cdf Eq. (13), then by statistical conditioning

$$F_{(\kappa_1/\kappa_2)}(t) = \mathbb{P}(\kappa_1 \le t\,\kappa_2) = \int_0^\infty \mathbb{P}(\kappa_1 \le t\omega)\, e^{-\omega}\, d\omega, \tag{14}$$

and an application of Eqs. (4)–(14) shows that the ratio has cdf Eq. (11) with an evaluation of the integral. This establishes the result in Corollary 3.1, as required.

3.2. Thresholds and the CUT

Based upon Corollary 3.1 the univariate threshold for the Pareto case is given by

$$\tau = \mathrm{Pfa}^{-1} - 1. \tag{15}$$

The threshold (Eq. (15)) illustrates the issues with the nonlinear mapping, as this threshold will be quite large for appropriate Pfa. Note that for a Pfa of 10^{-6}, $\tau = 10^6 - 1$. This threshold will increase as the Pfa decreases. In the Pareto setting, it is shown in Ref. [20] that an ideal detector has its threshold set via $\beta(\mathrm{Pfa})^{-1/\alpha}$. In the case where $\alpha = 4.7241$ and $\beta = 0.0446$ (which correspond to spiky clutter returns) and with the Pfa set to 10^{-6}, this threshold is 0.8312 by contrast. Thus the nonlinear mapping, in the process of compressing the original data series, can be used to achieve the CFAR property with Eq. (10), but detection performance may be unacceptable.

To explore this further, it is informative to examine the detection scheme in Eq. (10) when there is a target model present. Suppose Ξ is the CUT statistic, in the case where a target is present in the clutter, in the pretransformed data. Let $\hat{\Xi}$ be the CUT in the transformed domain, meaning the detector Eq. (10) when there is a target present so that T is the intensity measurement of a return signal and clutter in the complex domain. Then by applying the left-hand expression for Pareto random variables in Eq. (5), we can write

$$\hat{\Xi} = \alpha \left| \frac{\log(\Xi/\beta) - E_1}{E_2 - E_3} \right|, \tag{16}$$

where each E_j is an independent exponentially distributed random variable with unit mean. Then with an application of results from the proof of Corollary 3.1, since $|E_2 - E_3|$ has the same exponential distribution, one can apply statistical conditioning on E_1 and $|E_2 - E_3|$ to show that the distribution function of the transformed CUT is

$$\begin{aligned} F_{\hat{\Xi}}(t) &= \int_0^\infty \int_0^\infty e^{-\theta} e^{-\varphi}\, \mathbb{P}\left(\left| \log(\Xi/\beta) - \theta \right| \le \frac{\varphi t}{\alpha} \right) \mathrm{d}\theta \mathrm{d}\phi \\ &= \int_0^\infty \int_0^\infty e^{-\theta} e^{-\varphi}\, \mathbb{P}\left(\beta\, e^{\theta - \frac{\varphi t}{\alpha}} \le \Xi \le \beta\, e^{\theta + \frac{\varphi t}{\alpha}} \right) \mathrm{d}\theta \mathrm{d}\phi \\ &= \int_0^1 \int_0^1 \mathbb{P}\left(\beta\, x^{-1} y^{\frac{t}{\alpha}} \le \Xi \le \beta\, x^{-1} y^{-\frac{t}{\alpha}} \right) \mathrm{d}x \mathrm{d}y \\ &= \int_0^1 \int_0^1 F_\Xi\left(\beta\, x^{-1} y^{-\frac{t}{\alpha}} \right) - F_\Xi\left(\beta\, x^{-1} y^{\frac{t}{\alpha}} \right) \mathrm{d}x \mathrm{d}y, \end{aligned} \tag{17}$$

http://dx.doi.org/10.5772/65677

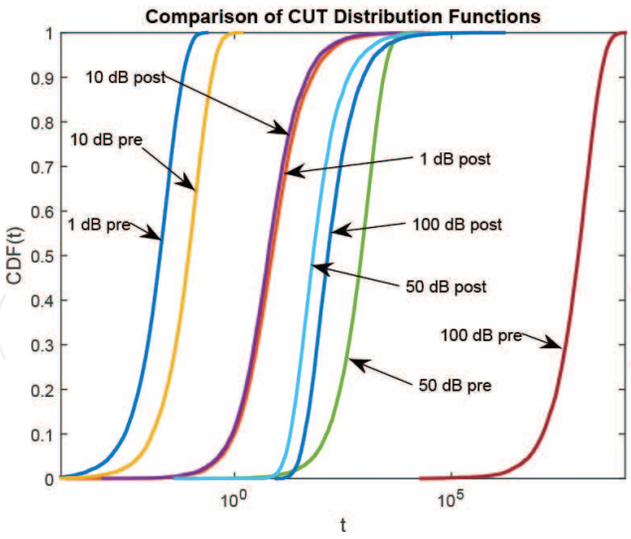

Figure 1. Comparison of CUT for the pretransformed data (denoted pre) and data processed via the nonlinear mapping (denoted post). The CUT is plotted for a Swerling 1 target model with a given SCR as indicated.

where the change of variables $x = e^{-\theta}$ and $y = e^{-\phi}$ has been applied. Thus the transformed CUT can be generated from the pretransformed CUT via Eq. (17). To examine this, **Figure 1** plots Eq. (17) in the case of a Swerling 1 target model embedded within Pareto distributed clutter with $\alpha = 4.7241$ and $\beta = 0.0446$. A Swerling I target model is essentially a bivariate Gaussian model, which is combined with the Pareto model by embedding the latter into a compound Gaussian process with inverse Gamma texture in the complex domain, and then taking modulus squared to produce the intensity measurement [20]. The distribution function of Ξ can also be found in Ref. [20] for the case of interest. **Figure 1** shows the pretransformed CUT as well as Eq. (17), in the cases where the signal to clutter (SCR) ratio is 1, 10, 50, and 100 dB. For the case of a 1 dB target model, the CUT has its range of potential values increased under the transformation. This is also the same for the 10 dB case. Interestingly, for the 50 dB and 100 dB cases, the situation is reversed. Hence, as the SCR increases, the nonlinear mapping suppresses the target SCR, reducing the range of admissible values for the transformed CUT. This suggests that although the nonlinear mapping removes unknown clutter parameters, it may also impede detection due to target suppression. If the threshold is set via Eq. (15), then it is clear from **Figure 1** that it will be very difficult to detect targets with a reasonably small Pfa. Hence, the new detection scheme must be combined with an integration process to rectify this.

4. Performance in homogeneous clutter

4.1. Methodology and data

In order to examine the performance of the proposed detection scheme (9), clutter is simulated under the assumption of a Pareto clutter model, which has been found to fit Defence Science and Technology Group's (DSTG's) real X-band maritime surveillance radar data sets. Ingara is an experimental X-band imaging radar which has provided real clutter for the analysis of detector performance [28]. A trial in 2004 produced a series of clutter sets that have been

analyzed from a statistical perspective in Ref. [29]. During the trial, the radar operated in a circular spotlight mode, surveying the same patch of the Southern Ocean at different azimuth and grazing angles. Additionally, the radar provided full polarimetric data. For the purposes of the numerical work to follow, focus is restricted to one particular data set. This is run 34683, at an azimuth angle of 225°, which is approximately in the up wind direction. Additionally, the numerical analysis focuses on the horizontal transmit and receive (HH) case.

For performance analysis in homogeneous clutter, the data is simulated with distributional parameters matched to those obtained from the Ingara data set. The data consists of 821 pulses with 1024 range compressed samples, from which maximum likelihood estimates of the distributional parameters can be obtained from the intensity measurements. Under the Pareto model assumption, the estimates are $\hat{\alpha} = 4.7241$ and $\hat{\beta} = 0.0446$.

As remarked previously, it is necessary to couple (10) with an integration scheme to enhance its performance. The integration scheme used for this purpose is binary integration, which is well-described in Ref. [30], and an application of it in a Pareto distributed clutter environment can be found in Ref. [31]. Such a process applies a series of $M \geq 1$ tests of Eq. (10), and then conclude that if at least S out of M return a detection result, then a target is likely to be present in the radar clutter [30], where $S \in \{1, 2, \ldots, M\}$. Selection of an appropriate S is outlined in Ref. [31]. Essentially, it is pointed out in Ref. [32] that for a specified univariate cumulative detection probability and false alarm rate and a fixed number of maximum binary integration returns M, there exists an optimal S which minimizes the required signal to clutter ratio, and maximizes the binary integration gain. This can be done visually or numerically by plotting the minimum SCR as a function of S, under the assumption of a certain signal model. This approach, and the analysis in Ref. [31], shows that in the current context, the choice of $S = 3$ with $M = 8$ should provide good results. Relative to the problem addressed in this chapter, applying binary integration with a linear threshold detector in the transformed clutter domain is not computationally expensive, and thus is seen as a reasonable solution.

If Pfa_{BI} denotes the Pfa for binary integration, then it can be expressed in terms of the univariate detection processes Pfa through the equation

$$\text{Pfa}_{\text{BI}} = \sum_{j=S}^{M} \binom{M}{j} \text{Pfa}^{j} (1 - \text{Pfa})^{M-j}. \tag{18}$$

The threshold τ is set via Eq. (18) coupled with the univariate Pfa from Eq. (9).

To simulate detection performance, the probability of detection (Pd) is estimated, using 10^6 Monte Carlo runs based upon a Swerling 1 target model assumed for the CUT. For each SCR, the binary integration process is run using $S = 3$ out of $M = 8$ binary integration. The motivation for these choices can be found in Ref. [31]. In order to assess the robustness of the detection scheme to interference, up to two interfering targets are inserted into the clutter measurements to give an indication of the performance with interference. Thus independent Swerling 1 targets, with interference to clutter ratio (ICR) of 1 dB, are applied to Z_1 (denoted Inter 1 in the plots), then to Z_2 (denoted Inter 2), and then to both Z_1 and Z_2 (denoted Inter 3) in the univariate decision rule in Eq. (9). A real spurious target may only appear in a subset of the clutter measurements and so this analysis of interference can be viewed as an upper bound on poor performance.

http://dx.doi.org/10.5772/65677

4.2. Receiver operating characteristic curves

Receiver operating characteristic (ROC) curves are used to examine the performance, which plots the probability of detection as a function of the false alarm probability, when the target in the CUT is at a fixed SCR. **Figures 2–4** provide examples of the performance of the new detector Eq. (10) with binary integration and compares it to the performance of some of the recently introduced detectors designed for operation in a Pareto clutter model environment. For a CUT Z and clutter range profile $Z_1, Z_2, \ldots, Z_N$, the Geometric Mean (GM) CFAR is

$$Z \underset{H_0}{\overset{H_1}{\gtrless}} \beta^{1-N\zeta} \prod_{j=1}^{N} Z_j^{\zeta}, \tag{19}$$

which is shown in Ref. [20] to have its threshold set via $\zeta = \text{Pfa}^{-1/N} - 1$. Similarly, an Order Statistic (OS)-CFAR has been analyzed in Ref [22], which is given by

$$Z \underset{H_0}{\overset{H_1}{\gtrless}} \beta^{1-v_j} Z_{(j)}^{v_j}, \tag{20}$$

which has its threshold multiplier v_j set via inversion of the Pfa equation given by

$$\text{Pfa} = \frac{N!}{(N-j)!} \frac{\Gamma(v_j + N - j + 1)}{\Gamma(v_j + N + 1)}, \tag{21}$$

where the OS index $1 \le j \le N$ and the notation v_j emphasizes the fact that v_j depends on the selected OS index j. Observe that both these decision rules require *a priori* knowledge of β. In order to provide a valid comparison with Eq. (10), these detectors have been applied with $N = 3$ and coupled with binary integration. Due to this, there are three choices available for j, corresponding to a minimum (denoted MIN, when $j = 1$), median (MED, $j = 2$), and maximum (MAX, $j = 3$).

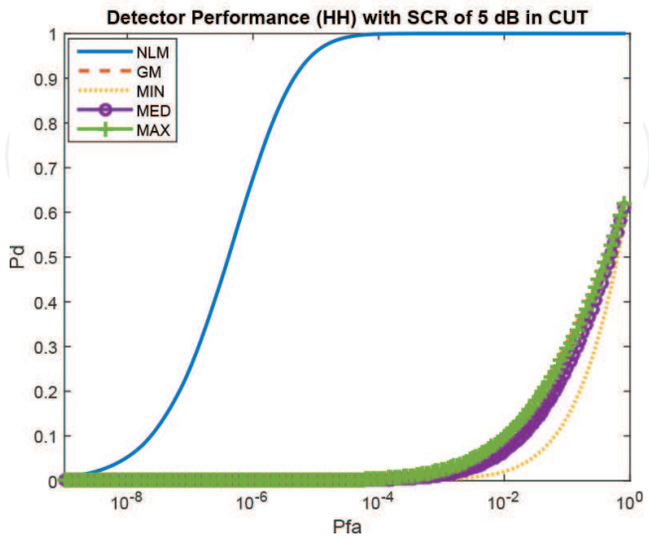

Figure 2. Comparison of detectors with a small target SCR.

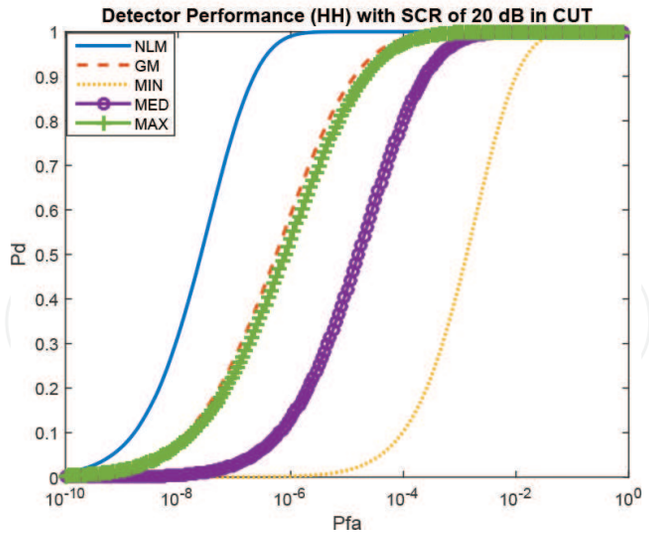

Figure 3. Detector performance with a larger SCR in the CUT.

Figure 2 compares the performance of these decision rules, where the detection process (10) coupled with binary integration is denoted as the nonlinear mapping (NLM). In this case, the CUT SCR is 5 dB, representing a small target. As can be observed, the new decision rule has superior performance. The same experiment is repeated in **Figure 3**, where the CUT SCR is 15 dB, and then it is increased to 20 dB in **Figure 4**. These results show that the new detection process has superior performance, while not requiring *a priori* knowledge of the Pareto scale parameter. These results validate the application of Eq. (10) to target detection in spiky X-band clutter with binary integration.

It is interesting to note that as M is increased, there is very little gain in performance. To demonstrate this, **Figure 5** repeats the same scenario in **Figure 4** except M has been increased to

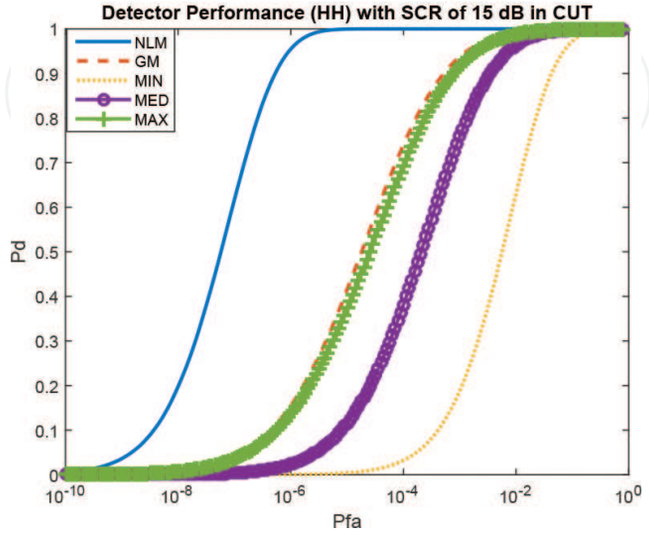

Figure 4. Decision rule performance with a CUT SCR of 20 dB.

http://dx.doi.org/10.5772/65677

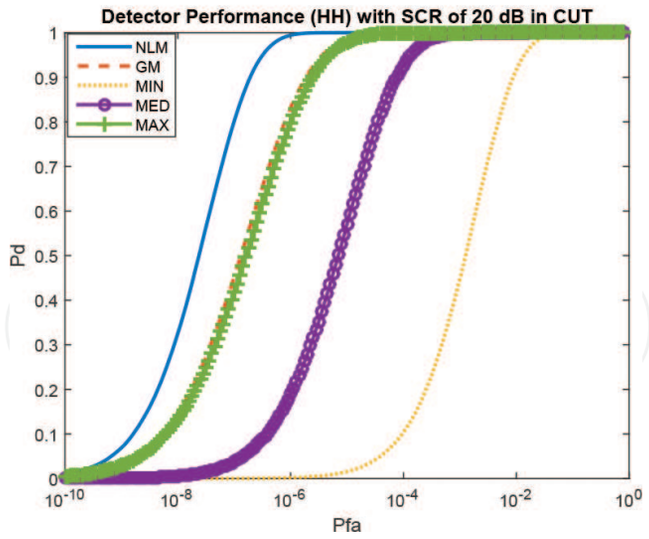

Figure 5. Decision rule performance with a CUT SCR of 20 dB, where the binary integration is $S = 3$ out of $M = 30$.

30. Comparing **Figures 4** and **5**, it is clear that there is very little gain. However, the computational complexity increases dramatically as M is increased. Hence, in a practical implementation of the binary integration process, it is more efficient to select M small.

4.3. Effect of interference

Next the cost of interference on the new decision rule is examined, and for brevity, only this decision rule is considered. **Figure 6** shows the case where the CUT has SCR of 5 dB, and the decision rule (10) coupled with binary integration is denoted BI, while the three interference cases are marked appropriately. Here we observe quite good performance that decreases with the interference. **Figure 7** shows the result of increasing the SCR in the CUT to 20 dB. The result is an expected detection performance improvement as shown.

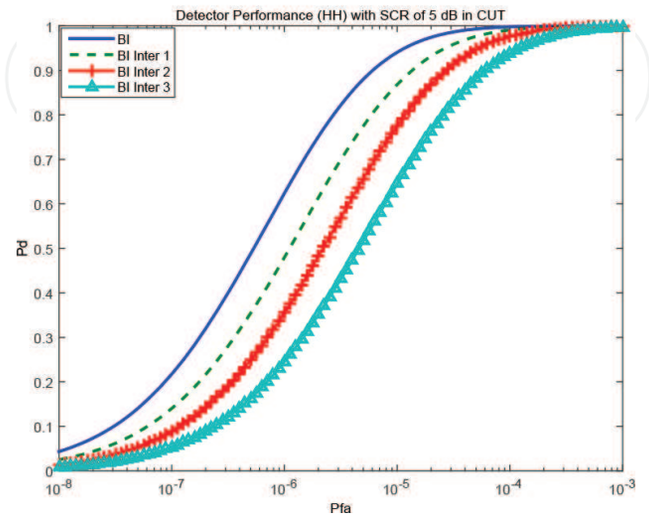

Figure 6. Performance of new detector when subjected to interference.

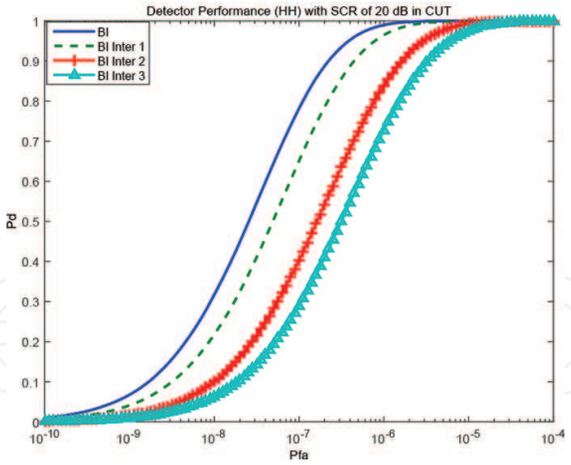

Figure 7. ROC for higher SCR with interference.

5. Performance in real data

As a final test of the proposed detection scheme, it was run directly on the Ingara data set under consideration, with the insertion of synthetic Swerling 1 target and interference as for the homogeneous case. A sliding window was run across the data sequentially, and detection performance was estimated by running the 3 out of 8 detection scheme, resulting in a run length of 840,672. The Ingara data is slightly correlated from cell to cell and so the detector Eq. (9), which has threshold set via an independence assumption, becomes a suboptimal decision rule. Detection performance under both clutter model assumptions is plotted on the same ROC curve to compare performance on the real data more easily. The same scenario is repeated as for the analysis under homogeneous independent clutter.

Figure 8 shows detection performance with the CUT SCR of 5 dB, while **Figure 9** repeats the same numerical experiment as for **Figure 8**, except the CUT has SCR of 20 dB. Comparing

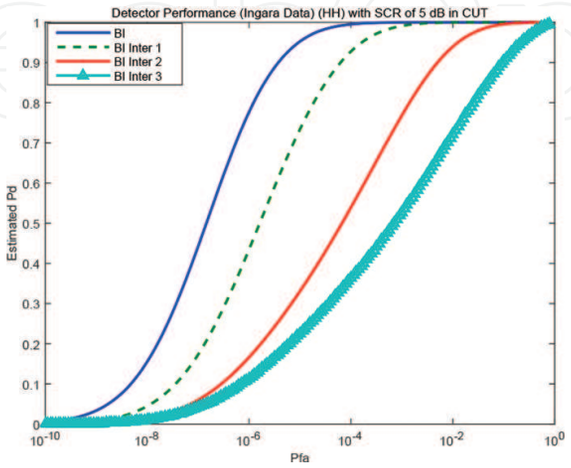

Figure 8. Performance of the detectors on the Ingara data directly.

http://dx.doi.org/10.5772/65677

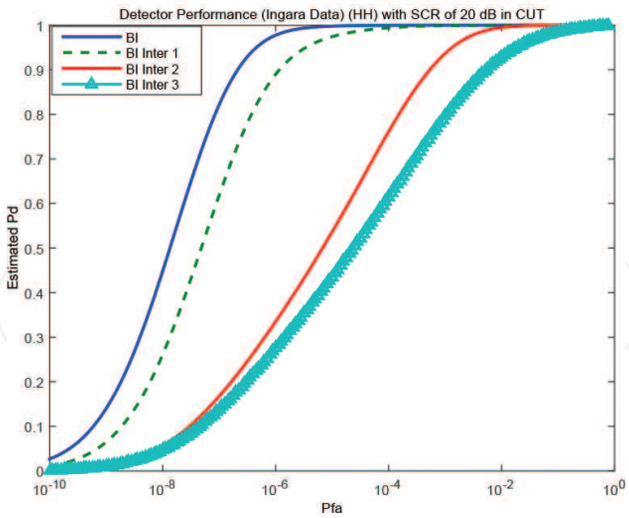

Figure 9. Second example of performance of the detectors on the Ingara data directly.

Figure 8 with **Figure 6** we observe that the effects of correlation are having an effect on the performance in real data. The new decision rule is designed to operate in independent homogeneous clutter returns, and so there is a serious variation in performance. The same situation is observed at a larger CUT SCR (comparing **Figures 9** and **7**).

6. Conclusions

A nonlinear transformation was introduced and shown to remove clutter parameter dependence for a class of statistical models. This was used to formulate a simple linear threshold detector in the transformed clutter domain. Due to issues with the magnitude of detection thresholds, it was necessary to couple the approach with binary integration.

Analysis of detection performance in simulated clutter showed good detection performance. Interference had a strong impact on performance as expected. When the detection process was applied directly to real data, similar results were observed. Nonetheless, the nonlinear transformation, coupled with binary integration, resulted in reasonable detection performance while guaranteeing the CFAR property is preserved.

Author details

Graham V. Weinberg

Address all correspondence to: Graham.Weinberg@defence.gov.au

National Security, Intelligence, Surveillance, Reconnaissance Division, Defence Science, Technology Group, Edinburgh, South Australia, Australia

References

[1] Minkler, G., Minkler, J.: CFAR: The Principles of Automatic Radar Detection in Clutter, Magellan, Baltimore, 1990.

[2] Finn, H. M., Johnson, R. S.: Adaptive Detection Model with Threshold Control as a Function of Spatially Sampled Clutter-Level Estimates, *RCA Review*, 1968, **29**, pp. 414–464.

[3] Nitzberg, R.: Low-Loss Almost Constant False-Alarm Rate Processors, *IEEE Transactions on Aerospace and Electronic Systems*, 1979, **AES-15**, pp. 719–723.

[4] Weiss, M.: Analysis of Some Modified Cell-Averaging CFAR Processors in Multiple-Target Situations, *IEEE Transactions on Aerospace and Electronic Systems*, 1982, **AES-18**, pp. 102–114.

[5] Rohling, H.: Radar CFAR Thresholding in Clutter and Multiple Target Situations, *IEEE Transactions on Aerospace and Electronic Systems*, 1983, **AES-19**, pp. 608–621

[6] Nitzberg, R.: Clutter Map CFAR Analysis, *IEEE Transactions on Aerospace and Electronic Systems*, 1986, **AES-22**, pp. 419–421.

[7] Gandhi, P. P., Kassam, S. A.: Analysis of CFAR Processors in Nonhomogeneous Background, *IEEE Transactions on Aerospace and Electronic Systems*, 1988, **24**, pp. 427–445.

[8] Chen, W.-S., Reed, I. S.: A New CFAR Detection Test for Radar, *Digital Signal Processing*, 1991, **1**, pp. 198–214.

[9] Al-Hussaini, E. K., El-Mashade, M. B.: Performance of Cell-Averaging and Order-Statistic CFAR Detectors Processing Correlated Sweeps for Multiple Interfering Targets, *Signal Processing*, 1996, **49**, pp. 111–118.

[10] Hamadouche, M, Barakat, M., Khodja, M.: Analysis of the Cutter Map CFAR in Weibull Clutter, *Signal Processing*, 2000, **80**, pp. 117–123.

[11] Laroussi, T., Barkat, M: Performance Analysis of Order-Statistic CFAR Detectors in Time Diversity Systems for Partially Correlated Chi-Square Targets and Multiple Target Situations: A Comparison, *Signal Processing*, 2006, **86**, pp. 1617–1631.

[12] Erfanian, S., Vakili, V. T.: Introducing Excision Switching-CFAR in K Distributed Sea Clutter, *Signal Processing*, 2009, **89**, pp. 1023–1031.

[13] Zhang, R., Sheng, W., Ma, X.: Improved Switching CFAR Detector for Non-Homogeneous Environments, *Signal Processing*, 2013, **93**, pp. 35–48.

[14] Zhang, R.-I., Sheng, W.-X., Ma, X.-F., Han, Y.-B.: Constant False Alarm Rate Detector based on the Maximal Reference Cell, *Digital Signal Processing*, 2013, **23**, pp. 1974–1988.

[15] Zaimbashi, A.: An Adaptive Cell Averaging-Based CFAR Detector for Interfering Targets and Clutter-Edge Situations, *Digital Signal Processing*, 2014, **31**, pp. 59–68.

[16] Balleri, A., Nehorai, A., Wang, J.: Maximum Likelihood Estimation for Compound-Gaussian Clutter with Inverse-Gamma Texture, *IEEE Transactions on Aerospace and Electronic Systems*, 2007, **43**, pp. 775–779.

[17] Farshchian, M., Posner. F. L.: The Pareto Distribution for Low Grazing Angle and High Resolution X-Band Sea Clutter, *IEEE Radar Conference*, 2010, pp. 789–793.

[18] Weinberg, G. V.: Assessing the Pareto Fit to High Resolution High Grazing Angle Sea Clutter, *IET Electronics Letters,* 2011, **47**, pp. 516–517.

[19] Sangston, K. J., Gini, F., Greco, M. S.: Coherent Radar Target Detection in Heavy-Tailed Compound Gaussian Clutter, *IEEE Transactions on Aerospace and Electronic Systems*, 2012, **48**, pp. 64–77.

[20] Weinberg, G. V.: Constant False Alarm Rate Detectors for Pareto Clutter Models, *IET Radar, Sonar and Navigation*, 2013, **7**, pp. 153–163.

[21] Weinberg, G. V.: General Transformation Approach for Constant False Alarm Rate Detector Development, *Digital Signal Processing*, 2014, **30**, pp. 15–26.

[22] Weinberg, G. V.: Constant False Alarm Rate Detection in Pareto Distributed Clutter: Further Results and Optimality Issues, *Contemporary Engineering Sciences*, 2014, **7**, pp. 231–261.

[23] Weinberg, G. V.: Management of Interference in Pareto CFAR Processes using Adaptive Test Cell Analysis, *Signal Processing*, 2014, **104**, pp. 264–273

[24] Weinberg, G.V.: Development of an Improved Minimum Order Statistic Detection Process for Pareto Distributed Clutter, *IET Radar, Sonar and Navigation*, 2015, **9**, pp. 19–30.

[25] Weinberg, G.V.: Examination of Classical Detection Schemes for Targets in Pareto Distributed Clutter: Do Classical CFAR Detectors Exist, as in the Gaussian Case?, *Multidimensional Systems and Signal Processing*, 2015, **26**, pp. 599–617.

[26] Beaumont, G. P.: Intermediate Mathematical Statistics, Chapman and Hall, London, 1980.

[27] Watts, S.: Radar Detection Prediction in Sea Clutter using the Compound K-Distribution Model, *IEE Proceedings, Part F*, 1985, **132**, pp. 613–620.

[28] Stacy, N. J. S., Burgess, M. P., Muller, M. R., Smith, R.: Ingara: An Integrated Airborne Imaging Radar System, *Proceedings of the International Geoscience and Remote Sensing Symposium*, 1996, pp. 1618–1620.

[29] Stacy, N., Crisp, D., Goh, A., Badger, D., Preiss, M.: Polarimetric Analysis of Fine Resolution X-Band Sea Clutter Data, *Proceedings of the International Geoscience and Remote Sensing Symposium,* 2005, pp. 2787–2790.

[30] Meng, X. W.: Performance Analysis of OS-CFAR with Binary Integration for Weibull Background, *IEEE Transactions on Aerospace and Electronic Systems,*, 2013, **49**, pp. 1357–1366.

[31] Weinberg, G. V., Kyprianou, R.: Optimised Binary Integration with Order Statistic CFAR in Pareto Distributed Clutter, *Digital Signal Processing*, 2015, **42**, pp. 50–60.

[32] Frey, T. L.: An Approximation for the Optimum Binary Integration Threshold for Swerling II Targets, *IEEE Transactions on Aerospace and Electronic Systems*, 1996, **32**, pp. 1181–1184.

IntechOpen